ISE

On computing the nonlinearity interval in parametric semidefinite optimization

Jonathan D. Hauenstein

Department of Applied and Computational Mathematics and Statistics, University of
Notre Dame, USA

Ali Mohammad-Nezhad

Department of Industrial and Systems Engineering, Lehigh University, USA

Tingting Tang

Department of Applied and Computational Mathematics and Statistics, University of
Notre Dame, USA

Tamás Terlaky

Department of Industrial and Systems Engineering, Lehigh University, USA

LEHIGH
UNIVERSITY.

On computing the nonlinearity interval in parametric semidefinite optimization

Jonathan D. Hauenstein

Department of Applied and Computational Mathematics and Statistics, University of Notre Dame, hauenstein@nd.edu

Ali Mohammad-Nezhad

Department of Industrial and Systems Engineering, Lehigh University, mohamm42@purdue.edu

Tingting Tang

Department of Applied and Computational Mathematics and Statistics, University of Notre Dame, ttang@nd.edu

Tamás Terlaky

Department of Industrial and Systems Engineering, Lehigh University, terlaky@lehigh.edu

This paper revisits the parametric analysis of semidefinite optimization problems with respect to the perturbation of the objective function along a fixed direction. We review the notions of invariancy set, nonlinearity interval, and transition point of the optimal partition, and we investigate their characterizations. We show that the continuity of the optimal set mapping, on the basis of Painlevé-Kuratowski set convergence, might fail on a nonlinearity interval. Furthermore, under a mild assumption, we prove that the set of transition points and the set of points at which the optimal set mapping is discontinuous are finite. We then present a methodology, stemming from numerical algebraic geometry, to efficiently compute nonlinearity intervals and transition points of the optimal partition. Finally, we support the theoretical results by applying our procedure to some numerical examples.

Key words: Parametric semidefinite optimization; Optimal partition; Nonlinearity interval; Numerical algebraic geometry

MSC2000 subject classification: Primary: 90C22; Secondary: 90C31, 90C51

1. Introduction Let $\mathbb{S}^n$ be the vector space of $n \times n$ symmetric matrices. Consider a parametric semidefinite optimization (SDO) problem

$$(\mathrm{P}_\epsilon) \qquad \inf_{X \in \mathbb{S}^n} \left\{ \langle C + \epsilon \bar{C}, X \rangle : \langle A^i, X \rangle = b_i, \quad i = 1, \ldots, m, \ X \succeq 0 \right\},$$

$$(\mathrm{D}_\epsilon) \qquad \sup_{(y,S) \in \mathbb{R}^m \times \mathbb{S}^n} \left\{ b^T y : \sum_{i=1}^m y_i A^i + S = C + \epsilon \bar{C}, \ S \succeq 0 \right\},$$

where $C, A_i \in \mathbb{S}^n$ for $i = 1, \ldots, m$, $b \in \mathbb{R}^m$, $\bar{C} \in \mathbb{S}^n$ is a fixed direction, the inner product is defined as $\langle C, X \rangle := \mathrm{tr}(CX)$, and $X \succeq 0$ means that the matrix X is symmetric and positive semidefinite. Let $v(\epsilon) \in \mathbb{R} \cup \{-\infty, \infty\}$ denote the optimal value of (P_ϵ). This yields a function $v : \mathbb{R} \to \mathbb{R} \cup \{-\infty, \infty\}$ which is the so-called *optimal value function*. Let $\mathcal{E} := \{\epsilon \in \mathbb{R} : v(\epsilon) > -\infty\}$ be the domain of $v(\epsilon)$.

The primal and dual optimal set mappings are defined as

$$\mathcal{P}^*(\epsilon) := \{X : \langle C + \epsilon \bar{C}, X \rangle = v(\epsilon), \ X \in \mathcal{P}(\epsilon)\},$$
$$\mathcal{D}^*(\epsilon) := \{(y,S) : b^T y = v(\epsilon), \ (y,S) \in \mathcal{D}(\epsilon)\},$$

where $\mathcal{P}(\epsilon)$ and $\mathcal{D}(\epsilon)$ denote the primal and dual feasible set mappings:

$$\mathcal{P}(\epsilon) := \{X : \langle A^i, X \rangle = b_i, \ i = 1, \ldots, m, \ X \succeq 0\},$$
$$\mathcal{D}(\epsilon) := \left\{ (y, S) : \sum_{i=1}^{m} y_i A^i + S = C + \epsilon \bar{C}, \ S \succeq 0 \right\}.$$

Note that $\mathcal{P}^*(\epsilon)$ or $\mathcal{D}^*(\epsilon)$ might be empty for some $\epsilon \in \mathcal{E}$. To avoid trivialities, we make the following assumption throughout this paper:

ASSUMPTION 1. *The interior point condition holds for both* (P_ϵ) *and* (D_ϵ) *at* $\epsilon = 0$, *i.e., there exists a feasible* $\left(X^\circ(0), y^\circ(0), S^\circ(0)\right) \in \mathcal{P}^*(0) \times \mathcal{D}^*(0)$ *such that* $X^\circ(0), S^\circ(0) \succ 0$, *where* $\succ 0$ *means positive definite.*

Assumption 1 implies that $\mathcal{E}$ is nonempty and non-singleton, and that $v(\epsilon)$ is proper and concave on $\mathcal{E}$ [8, Lemma 2.2]. The concavity of $v(\epsilon)$ yields that $\mathcal{E}$ is a closed, possibly unbounded, interval [8, Lemma 2.2] and that $v(\epsilon)$ is continuous on $\mathrm{int}(\mathcal{E})$ [11, Corollary 2.109].

REMARK 1. Assumption 1 is equivalent to the existence of a strictly feasible solution $\left(X^\circ(\epsilon), y^\circ(\epsilon), S^\circ(\epsilon)\right)$ at every $\epsilon \in \mathrm{int}(\mathcal{E})$ [19, Lemma 3.1], where $\mathrm{int}(.)$ denotes the interior of a convex set.

Hence, for all $\epsilon \in \mathrm{int}(\mathcal{E})$, Assumption 1 ensures that strong duality holds and that the optimal sets $\mathcal{P}^*(\epsilon)$ and $\mathcal{D}^*(\epsilon)$ are nonempty and compact. In this paper, by strong duality we mean that the optimal values of (P_ϵ) and (D_ϵ) are both attained and the duality gap is zero, see e.g., [11, Theorem 5.81]. In particular, the optimality conditions for (P_ϵ) and (D_ϵ) can be written as

$$
\begin{aligned}
\langle A^i, X \rangle &= b_i, & i = 1, \ldots, m, \\
\sum_{i=1}^{m} y_i A^i + S &= C + \epsilon \bar{C}, \\
XS &= 0, \\
X, S &\succeq 0,
\end{aligned}
\tag{1}
$$

where $XS = 0$ denotes the complementarity condition. Furthermore, Assumption 1 guarantees the existence of a so-called maximally complementary optimal solution for every $\epsilon \in \mathrm{int}(\mathcal{E})$.

DEFINITION 1. An optimal solution $\left(X^*(\epsilon), y^*(\epsilon), S^*(\epsilon)\right)$ is called *maximally complementary* if

$$X^*(\epsilon) \in \mathrm{ri}\left(\mathcal{P}^*(\epsilon)\right) \quad \text{and} \quad \left(y^*(\epsilon), S^*(\epsilon)\right) \in \mathrm{ri}\left(\mathcal{D}^*(\epsilon)\right),$$

where $\mathrm{ri}(.)$ denotes the relative interior of a convex set. A maximally complementary optimal solution $\left(X^*(\epsilon), y^*(\epsilon), S^*(\epsilon)\right)$ is called *strictly complementary* if $X^*(\epsilon) + S^*(\epsilon) \succ 0$.

For any fixed $\epsilon \in \mathrm{int}(\mathcal{E})$, $\mathrm{rank}\left(X^*(\epsilon)\right) + \mathrm{rank}\left(S^*(\epsilon)\right)$ is maximal on $\mathcal{P}^*(\epsilon) \times \mathcal{D}^*(\epsilon)$, see e.g., [15, Lemma 2.3]. Even though a strictly complementary optimal solution may fail to exist, a maximally complementary optimal solution always exists under Assumption 1.

In practice, given a fixed ϵ, (P_ϵ) and (D_ϵ) can be efficiently solved in polynomial time using a primal-dual path-following interior point method (IPM), see [32]. A primal-dual path following IPM generates a sequence of solutions whose accumulation points are maximally complementary optimal solutions [21].

1.1. Optimal partition For SDO, the optimal partition information can be leveraged to establish sensitivity analysis results. The optimal partition provides a characterization of the optimal set, and it is uniquely defined for any instance of an SDO problem which satisfies strong

duality [15]. For a fixed $\epsilon \in \text{int}(\mathcal{E})$, let $\big(X^*(\epsilon), y^*(\epsilon), S^*(\epsilon)\big) \in \text{ri}\big(\mathcal{P}^*(\epsilon) \times \mathcal{D}^*(\epsilon)\big)$ be a maximally complementary optimal solution, and let $\mathcal{B}(\epsilon) := \mathcal{R}\big(X^*(\epsilon)\big)$, $\mathcal{N}(\epsilon) := \mathcal{R}\big(S^*(\epsilon)\big)$, and $\mathcal{T}(\epsilon) := \big(\mathcal{R}\big(X^*(\epsilon)\big) + \mathcal{R}\big(S^*(\epsilon)\big)\big)^{\perp}$, where $\mathcal{R}(.)$ is the column space and $\perp$ denotes the orthogonal complement of a subspace. Then the triple $\big(\mathcal{B}(\epsilon), \mathcal{T}(\epsilon), \mathcal{N}(\epsilon)\big)$ is called the *optimal partition* of (P_ϵ) and (D_ϵ). Note that the subspaces $\mathcal{R}\big(X^*(\epsilon)\big)$ and $\mathcal{R}\big(S^*(\epsilon)\big)$ are orthogonal by the complementarity condition in (1). Further, the optimal partition $\big(\mathcal{B}(\epsilon), \mathcal{T}(\epsilon), \mathcal{N}(\epsilon)\big)$ is independent of the choice of a maximally complementary optimal solution [15, Lemma 2.3(i)].

1.2. Related works Sensitivity analysis along a fixed direction has been extensively studied in optimization theory and was originally introduced for linear optimization (LO) and linearly constrained quadratic optimization (LCQO) problems in [1, 8, 27]. Sensitivity analysis of nonlinear optimization problems was studied by Fiacco [17] and Fiacco and McCormick [16] using the implicit function theorem [36]. Their analysis was based on linear independence constraint qualification, second-order sufficient condition, and the strict complementarity condition. Furthermore, Fiacco [17] showed how to compute/approximate the partial derivatives of a locally optimal solution. Robinson [35] removed the reliance on the strict complementarity condition by imposing a strong second-order sufficient condition. Kojima [29] removed the dependence on the strict complementarity condition by invoking the degree theory of a continuous map, see e.g., [33]. See [18] for a survey of classical results.

A comprehensive treatment of directional and differential stability of nonlinear SDO problems is given by Bonnans and Shapiro [10, 11], see also [9, 38]. The study of sensitivity analysis based on the optimal partition approach was initiated by Adler and Monteiro [1] and Jansen et al. [27] for LO and then extended for LCQO, SDO, and linear conic optimization by Berkelaar et al. [8], Goldfarb and Scheinberg [19], and Yildirim [43], respectively. Recently, the second and fourth authors [30] introduced the concepts of a nonlinearity interval and a transition point for the optimal partition of (P_ϵ) and (D_ϵ) to investigate the sensitivity of the optimal partition and the approximation of the optimal partition with respect to ϵ.

1.3. Contributions A parametric SDO problem was initially studied in [19, 30]. Based on the notion of an invariancy set, which might be either a singleton or an open interval, from [19, 30] and the notions of nonlinearity interval and transition point from [30], we present a methodology for the identification of the optimal partitions on the entire $\text{int}(\mathcal{E})$. An invariancy interval is an open subinterval of $\text{int}(\mathcal{E})$ on which the optimal partition is invariant with respect to ϵ. A nonlinearity interval is an open maximal length subinterval of $\text{int}(\mathcal{E})$ on which the rank of maximally complementary optimal solutions $X^*(\epsilon)$ and $S^*(\epsilon)$ stay constant, while the optimal partition varies with ϵ. A transition point is a singleton invariancy set which does not belong to a nonlinearity interval. To the best of our knowledge, this is the first comprehensive methodology for the computation of nonlinearity intervals and transition points in $\text{int}(\mathcal{E})$.

Our main contributions are 1) the study of continuity of optimal set mapping on a nonlinearity interval, 2) algebraic interpretation of transition points of the optimal partition, and 3) a numerical procedure for the computation of nonlinearity intervals and transition points. Using continuity arguments on the basis of Painlevé-Kuratowski set convergence, we provide sufficient conditions under which the set of transition points has empty interior, see Lemma 2, and a nonlinearity interval exists, see Lemma 3. We analyze the continuity of the optimal set mapping and show that continuity may fail on a nonlinearity interval, see problem (8). Furthermore, we show that even a continuous selection [37, Chapter 5(J)] through the relative interior of the optimal sets might fail to exist, see problem (10). The second part of this paper investigates the computation of nonlinearity intervals and transition points of the optimal partition. Under a mild assumption, we show that the set of transition points and the set of points at which the optimal set mapping fails to be

continuous relative to $\mathrm{int}(\mathcal{E})$ are finite, see Theorem 2. Using numerical algebraic geometry, we then present a methodology to partition $\mathrm{int}(\mathcal{E})$ into the finite union of invariancy intervals, nonlinearity intervals, and transition points, see Algorithms 1 through 4.

Besides sensitivity analysis purposes and their economical interpretations, the identification of a nonlinearity interval is important from practical perspectives. For example, in order to approximate the optimal value function on a neighborhood of a given ϵ, one needs to utilize samples from the same nonlinearity interval containing ϵ. Cifuentes et al. [13] studied the local stability of SDO relaxations for polynomial and semi-algebraic optimization problems with emphasis on a notion similar to a nonlinearity interval.

1.4. Organization of the paper   The rest of this paper is organized as follows. In Section 2, we investigate the continuity of the feasible and optimal set mappings at a given $\epsilon \in \mathrm{int}(\mathcal{E})$ relative to $\mathrm{int}(\mathcal{E})$. In Section 3, we study the sensitivity of the optimal partition with respect to ϵ. Further, we use continuity arguments to partially characterize nonlinearity intervals and transition points, and we investigate the continuity of the optimal set mapping on a nonlinearity interval. In Section 4, we present an algorithm to partition $\mathrm{int}(\mathcal{E})$ into invariancy intervals, nonlinearity intervals, and transition points of the optimal partition. Our numerical experiments are presented in Section 5. Finally, we present remarks and topics for future research in Section 6.

Notation   Throughout this paper, $\mathbb{S}_+^n$ denotes the cone of $n \times n$ symmetric positive semidefinite matrices. Associated with a symmetric matrix, $\lambda_{\min}(X)$ denotes the smallest eigenvalue of X, $\Lambda(X)$ serves as the diagonal matrix of the eigenvalues, and $\mathrm{svec}(X)$ denotes a linear mapping stacking the upper triangular part of a symmetric matrix, in which the off-diagonal entries are multiplied by $\sqrt{2}$, i.e.,

$$\mathrm{svec}(X) := \left(X_{11}, \sqrt{2}X_{12}, \ldots, \sqrt{2}X_{1n}, X_{22}, \sqrt{2}X_{23}, \ldots, \sqrt{2}X_{2n}, \ldots, X_{nn}\right)^T.$$

For any two square matrices K_1 and K_2 and a symmetric matrix H, the *symmetric Kronecker product*, denoted by $\otimes_s$, is defined as

$$(K_1 \otimes_s K_2)\,\mathrm{svec}(H) := \frac{1}{2}\,\mathrm{svec}\left(K_2 H K_1^T + K_1 H K_2^T\right),$$

see e.g., [15] for more details. Finally, for a given $\epsilon \in \mathrm{int}(\mathcal{E})$, a maximally complementary optimal solution is denoted by $\left(X^*(\epsilon), y^*(\epsilon), S^*(\epsilon)\right)$.

2. Continuity of the feasible set and optimal set mappings   This section investigates the continuity of the primal and dual feasible set mappings and the outer semicontinuity of the primal and dual optimal set mappings for (P_ϵ) and (D_ϵ). We adopt the notions and definitions from [37].

Let $\mathbb{R}^q$ and $\mathbb{R}^l$ be finite-dimensional Euclidean spaces. A mapping $\Phi(\xi): \mathbb{R}^q \rightrightarrows \mathbb{R}^l$ is called a *set-valued mapping* if it assigns a subset of $\mathbb{R}^l$ to each element of $\mathbb{R}^q$. The domain of a set-valued mapping $\Phi(\xi)$ is

$$\mathrm{dom}(\Phi) := \{\xi : \Phi(\xi) \neq \emptyset\},$$

and the range of $\Phi(\xi)$ is defined as

$$\mathrm{range}(\Phi) := \{\nu : \exists\,\xi \text{ s.t. } \nu \in \Phi(\xi)\}.$$

The following discussion concisely reviews the continuity of a set-valued mapping on the basis of Painlevé-Kuratowski set convergence, see [37, Chapters 4 and 5] for more details. Let $\mathbb{N}$ be the set

of natural numbers, $\mathcal{J}$ denote the collection of subsets $J \subseteq \mathbb{N}$ such that $\mathbb{N} \setminus J$ is finite, and $\mathcal{J}_\infty$ be the collection of all infinite subsets of $\mathbb{N}$. For a sequence $\{\mathcal{C}_k\}_{k=1}^\infty$ of subsets of $\mathbb{R}^l$, the *outer* and *inner* limits are defined, respectively, as

$$\limsup_{k \to \infty} \mathcal{C}_k := \left\{ \nu : \exists\ J \in \mathcal{J}_\infty,\ \exists\ \nu_k \in \mathcal{C}_k, (k \in J) \text{ with } \nu_k \xrightarrow{J} \nu \right\},$$
$$\liminf_{k \to \infty} \mathcal{C}_k := \left\{ \nu : \exists\ J \in \mathcal{J},\ \exists\ \nu_k \in \mathcal{C}_k, (k \in J) \text{ with } \nu_k \xrightarrow{J} \nu \right\},$$

where $\nu_k \xrightarrow{J} \nu$ means that $\lim_{k \in J} \nu_k = \nu$. Let $\mathcal{X}$ be a subset of $\mathbb{R}^q$ containing $\bar{\xi}$. A set-valued mapping $\Phi(\xi)$ is called *outer semicontinuous* at $\bar{\xi}$ relative to $\mathcal{X}$ if $\limsup_{\xi \to \bar{\xi}} \Phi(\xi) \subseteq \Phi(\bar{\xi})$ and *inner semicontinuous* at $\bar{\xi}$ relative to $\mathcal{X}$ if $\liminf_{\xi \to \bar{\xi}} \Phi(\xi) \supseteq \Phi(\bar{\xi})$, where

$$\limsup_{\xi \to \bar{\xi}} \Phi(\xi) := \left\{ \nu : \exists\ \{\xi_k\}_{k=1}^\infty \subseteq \mathcal{X} \text{ with } \xi_k \to \bar{\xi},\ \exists\ \nu_k \to \nu \text{ with } \nu_k \in \Phi(\xi_k) \right\},$$
$$\liminf_{\xi \to \bar{\xi}} \Phi(\xi) := \left\{ \nu : \forall\ \{\xi_k\}_{k=1}^\infty \subseteq \mathcal{X} \text{ with } \xi_k \to \bar{\xi},\ \exists\ \nu_k \to \nu \text{ with } \nu_k \in \Phi(\xi_k) \right\}. \tag{2}$$

When $\mathcal{X} = \mathbb{R}^q$, we simply call $\Phi(\xi)$ outer or inner semicontinuous at $\bar{\xi}$.

DEFINITION 2. A set-valued mapping $\Phi(\xi)$ is *Painlevé-Kuratowski continuous* at $\bar{\xi}$ relative to $\mathcal{X}$ if it is both outer and inner semicontinuous at $\bar{\xi}$ relative to $\mathcal{X}$.

In our setting, outer and inner semicontinuity agree with the notions of closedness and openness of a point-to-set map in [26], see also [37, Theorem 5.7(c)] and [26, Corollary 1.1].

We show the continuity of the feasible set mapping and the outer semicontinuity of the optimal set mapping relative to $\text{int}(\mathcal{E})$. Trivially, $\mathcal{P}(\epsilon) : \mathbb{R} \rightrightarrows \mathbb{S}^n$ is continuous since it remains invariant with respect to ϵ. Furthermore, the continuity of $\mathcal{D}(\epsilon) : \mathbb{R} \rightrightarrows \mathbb{R}^m \times \mathbb{S}^n$ relative to $\text{int}(\mathcal{E})$ follows from [26, Theorems 10 and 12], where $\mathcal{D}(\epsilon) = \emptyset$ for every $\epsilon \in \mathbb{R} \setminus \mathcal{E}$. For the sake of completeness, we provide a proof for our special case here. Let $\mathcal{D}^y(\epsilon) : \mathbb{R} \rightrightarrows \mathbb{R}^m$ be a set-valued mapping defined by

$$\mathcal{D}^y(\epsilon) := \left\{ y \in \mathbb{R}^m :\ C + \epsilon \bar{C} - \sum_{i=1}^m y_i A^i \succeq 0 \right\}.$$

Now, the following result is in order.

LEMMA 1. *Under Assumption 1, the set-valued mapping $\mathcal{D}^y(\epsilon)$ and thus $\mathcal{D}(\epsilon)$ are continuous relative to $\text{int}(\mathcal{E})$.*

Proof Since $\mathbb{S}^n_+$ is a closed convex cone and $\text{int}(\mathcal{E}) \subseteq \text{dom}(\mathcal{D}^y)$, it follows that $\mathcal{D}^y(\epsilon)$ is outer semicontinuous relative to $\text{int}(\mathcal{E})$, see e.g., [37, Example 5.8]. Hence, it only remains to show that $\mathcal{D}^y(\epsilon)$ is inner semicontinuous at every $\epsilon' \in \text{int}(\mathcal{E})$.

Let $\bar{y} \in \mathcal{D}^y(\epsilon')$ such that $C + \epsilon' \bar{C} - \sum_{i=1}^m \bar{y}_i A^i \succ 0$ and $\hat{y} \in \mathcal{D}^y(\epsilon')$ such that $\hat{S} := C + \epsilon' \bar{C} - \sum_{i=1}^m \hat{y}_i A^i$ has at least one zero eigenvalue. The case when $\hat{S} \succ 0$ is trivial. Given a sequence $\{\epsilon_k\}_{k=1}^\infty$ with $\epsilon_k \to \epsilon'$, we will construct a convergent sequence $y_k \to \hat{y}$ so that $C + \epsilon_k \bar{C} - \sum_{i=1}^m (y_k)_i A^i \succeq 0$ for all sufficiently large values of k.

Define $y_k = (1 - \alpha_k)\hat{y} + \alpha_k \bar{y}$. Note that $C + \epsilon_k \bar{C} - \sum_{i=1}^m (y_k)_i A^i \succeq 0$ holds if

$$(1 - \alpha_k)\left(C + \epsilon_k \bar{C} - \sum_{i=1}^m \hat{y}_i A^i \right) + \alpha_k \left(C + \epsilon_k \bar{C} - \sum_{i=1}^m \bar{y}_i A^i \right) \succeq 0. \tag{3}$$

If $0 \leq \alpha_k \leq 1$, then (3) holds if

$$(1 - \alpha_k)\lambda_{\min}\Big(C + \epsilon_k \bar{C} - \sum_{i=1}^{m} \hat{y}_i A^i\Big) + \alpha_k \lambda_{\min}\Big(C + \epsilon_k \bar{C} - \sum_{i=1}^{m} \bar{y}_i A^i\Big) \geq 0,$$

which is equivalent to

$$\alpha_k \geq \frac{-\lambda_{\min}\big(C + \epsilon_k \bar{C} - \sum_{i=1}^{m} \hat{y}_i A^i\big)}{\lambda_{\min}\big(C + \epsilon_k \bar{C} - \sum_{i=1}^{m} \bar{y}_i A^i\big) - \lambda_{\min}\big(C + \epsilon_k \bar{C} - \sum_{i=1}^{m} \hat{y}_i A^i\big)}$$

for sufficiently large k, since the denominator has to be positive. Letting $\alpha_k := \max\{\rho_k, 0\}$, where

$$\rho_k := \frac{-\lambda_{\min}\big(C + \epsilon_k \bar{C} - \sum_{i=1}^{m} \hat{y}_i A^i\big)}{\lambda_{\min}\big(C + \epsilon_k \bar{C} - \sum_{i=1}^{m} \bar{y}_i A^i\big) - \lambda_{\min}\big(C + \epsilon_k \bar{C} - \sum_{i=1}^{m} \hat{y}_i A^i\big)},$$

we have $\rho_k \to 0$ and $y_k \in \mathcal{D}^y(\epsilon_k)$ for sufficiently large k since $0 \leq \alpha_k \leq 1$ and $\alpha_k \to 0$. This completes the proof for the continuity of $\mathcal{D}^y(\epsilon)$ relative to $\text{int}(\mathcal{E})$. The continuity of $\mathcal{D}(\epsilon)$ is then immediate from $S = C + \epsilon \bar{C} - \sum_{i=1}^{m} y_i A^i$. $\square$

As a result of Lemma 1, we can show that $\mathcal{P}^*(\epsilon) : \mathbb{R} \rightrightarrows \mathbb{S}^n$ and $\mathcal{D}^*(\epsilon) : \mathbb{R} \rightrightarrows \mathbb{R}^m \times \mathbb{S}^n$ are outer semicontinuous relative to $\text{int}(\mathcal{E})$, see e.g., [26, Theorem 8]. All this implies that for any $\epsilon' \in \text{int}(\mathcal{E})$ and any sequence $\epsilon_k \to \epsilon'$ we have

$$\liminf_{k \to \infty} \mathcal{P}^*(\epsilon_k) \subseteq \limsup_{k \to \infty} \mathcal{P}^*(\epsilon_k) \subseteq \mathcal{P}^*(\epsilon') \quad \text{and} \quad \liminf_{k \to \infty} \mathcal{D}^*(\epsilon_k) \subseteq \limsup_{k \to \infty} \mathcal{D}^*(\epsilon_k) \subseteq \mathcal{D}^*(\epsilon').$$

However, $\mathcal{P}^*(\epsilon)$ and $\mathcal{D}^*(\epsilon)$ are not necessarily inner semicontinuous relative to $\text{int}(\mathcal{E})$ as shown in Example 1, where the optimal set is multiple-valued at $\epsilon = \frac{1}{2}$ but single-valued everywhere else in a neighborhood of $\frac{1}{2}$. Nevertheless, the set of points at which $\mathcal{P}^*(\epsilon)$ or $\mathcal{D}^*(\epsilon)$ fails to be continuous relative to $\text{int}(\mathcal{E})$ is of *first category* in $\text{int}(\mathcal{E})$, i.e., it is the union of countably many nowhere dense sets in $\text{int}(\mathcal{E})$, see e.g., [31]. This directly follows from the outer semicontinuity of the optimal set mapping relative to $\text{int}(\mathcal{E})$ and Theorem 5.55 in [37]. All this yields the following result.

THEOREM 1. *The set of points at which $\mathcal{P}^*(\epsilon)$ or $\mathcal{D}^*(\epsilon)$ fails to be continuous relative to $\text{int}(\mathcal{E})$ has empty interior.*

Proof Since $\text{int}(\mathcal{E})$ is a Baire subset of $\mathbb{R}$ [31, Lemma 48.4], every first category subset of $\text{int}(\mathcal{E})$ has empty interior. $\square$

As a consequence of Theorem 1, every open subset of $\text{int}(\mathcal{E})$ contains a point at which both $\mathcal{P}^*(\epsilon)$ and $\mathcal{D}^*(\epsilon)$ are continuous relative to $\text{int}(\mathcal{E})$.

3. Sensitivity of the optimal partition We briefly review the notions of an invariancy interval, nonlinearity interval, and a transition point from [30]. Let $\pi(\epsilon) := \big(\mathcal{B}(\epsilon), \mathcal{T}(\epsilon), \mathcal{N}(\epsilon)\big)$ denote the subspaces of the optimal partition at ϵ, and let

$$Q_\epsilon := \big(Q_{\mathcal{B}(\epsilon)}, Q_{\mathcal{T}(\epsilon)}, Q_{\mathcal{N}(\epsilon)}\big)$$

be an orthonormal basis partitioned according to the subspaces of the optimal partition.

DEFINITION 3 ([19, 30]). An *invariancy set* is a subset $\mathcal{I}_{\text{inv}}$ of $\text{int}(\mathcal{E})$ on which $\pi(\epsilon)$ is invariant for all $\epsilon \in \mathcal{I}_{\text{inv}}$. A non-singleton $\mathcal{I}_{\text{inv}}$ is called an *invariancy interval*. Otherwise, $\mathcal{I}_{\text{inv}}$ is called a *singleton invariancy set*.

Indeed, a non-singleton invariancy set is proven to be an open, possibly unbounded, subinterval of $\text{int}(\mathcal{E})$ [30, Section 3.1]. The boundary points of an invariancy set, containing a given $\bar{\epsilon}$, can be efficiently computed by solving a pair of auxiliary SDO problems [19, Lemma 4.1]:

$$
\begin{aligned}
\alpha_{\text{inv}}(\beta_{\text{inv}}) := \inf(\sup) \quad & \epsilon \\
\text{s.t.} \quad & \sum_{i=1}^{m} y_i A^i + Q_{\mathcal{N}(\bar{\epsilon})} U_S Q_{\mathcal{N}(\bar{\epsilon})}^T = C + \epsilon \bar{C}, \\
& U_S \succ 0,
\end{aligned}
\tag{4}
$$

where we might have $\alpha_{\text{inv}} = -\infty$, $\beta_{\text{inv}} = \infty$, or both. If $\alpha_{\text{inv}} < \bar{\epsilon} < \beta_{\text{inv}}$ holds, then $\bar{\epsilon}$ belongs to an invariancy interval. Otherwise, $\bar{\epsilon}$ is a singleton invariancy set which either belongs to a nonlinearity interval, or it is a transition point, as formally defined in Definitions 4 and 5.

DEFINITION 4 (DEFINITION 3.6 IN [30]). A *nonlinearity interval* is an open maximal subinterval $\mathcal{I}_{\text{non}}$ of $\text{int}(\mathcal{E})$ on which both $\text{rank}\big(X^*(\epsilon)\big)$ and $\text{rank}\big(S^*(\epsilon)\big)$ are constant while $\pi(\epsilon)$ varies with ϵ.

DEFINITION 5 (DEFINITION 3.5 IN [30]). A singleton invariancy set $\{\bar{\epsilon}\} \subset \text{int}(\mathcal{E})$ is called a *transition point* if for every $\delta > 0$, there exists $\epsilon \in (\bar{\epsilon} - \delta, \bar{\epsilon} + \delta)$ such that

$$
\text{rank}\big(X^*(\epsilon)\big) \neq \text{rank}\big(X^*(\bar{\epsilon})\big) \quad \text{or} \quad \text{rank}\big(S^*(\epsilon)\big) \neq \text{rank}\big(S^*(\bar{\epsilon})\big).
\tag{5}
$$

REMARK 2. Both the primal and dual optimal sets must vary with ϵ on a nonlinearity interval. Otherwise, one would get an invariancy interval [30, Lemma 3.3 and Remark 5]. Indeed, a nonlinearity interval can be thought of as the union of infinitely many singleton invariancy sets on which both $\text{rank}\big(X^*(\epsilon)\big)$ and $\text{rank}\big(S^*(\epsilon)\big)$ stay constant.

Since the domain $\mathcal{E}$ may be unbounded, a nonlinearity interval $\mathcal{I}_{\text{non}}$ may be unbounded too. Furthermore, a boundary point of an invariancy or a nonlinearity interval must be a transition point, since (5) always holds at a boundary point, see also [30, Remark 5]. Lemma 2 indicates that under an extra condition, the converse of this statement is true as well, i.e., a transition point must be a boundary point of an invariancy or a nonlinearity interval.

LEMMA 2. *Assume that the set of points at which $\mathcal{P}^*(\epsilon)$ or $\mathcal{D}^*(\epsilon)$ fails to be continuous relative to $\text{int}(\mathcal{E})$ is finite. Then the set of transition points in $\text{int}(\mathcal{E})$ has empty interior.*

Proof To reach a contradiction, suppose that there exists a subset $\mathcal{I} \subseteq \text{int}(\mathcal{E})$ with $\text{int}(\mathcal{I}) \neq \emptyset$ such that ϵ is a transition point for every $\epsilon \in \mathcal{I}$. By the assumption, there must exist $\bar{\epsilon} \in \text{int}(\mathcal{I})$ and $\varsigma > 0$ such that both $\mathcal{P}^*(\epsilon)$ and $\mathcal{D}^*(\epsilon)$ are continuous on $(\bar{\epsilon} - \varsigma, \bar{\epsilon} + \varsigma)$, and

$$
\text{rank}\big(X^*(\bar{\epsilon})\big) \leq \text{rank}\big(X^*(\epsilon)\big) \quad \text{and} \quad \text{rank}\big(S^*(\bar{\epsilon})\big) \leq \text{rank}\big(S^*(\epsilon)\big)
$$

hold with at least one strict inequality for every $\epsilon \in (\bar{\epsilon} - \varsigma, \bar{\epsilon} + \varsigma)$. Then choosing $\bar{\epsilon} := \epsilon$ and applying this argument infinitely many times with a small enough $\varsigma > 0$ and an $\epsilon \in (\bar{\epsilon} - \varsigma, \bar{\epsilon} + \varsigma)$, we arrive at a contradiction, since each iteration increases $\text{rank}\big(X^*(\epsilon)\big)$ or $\text{rank}\big(S^*(\epsilon)\big)$ at least by 1. $\quad\square$

Under the condition of Lemma 2, the union of invariancy and nonlinearity intervals is dense in $\text{int}(\mathcal{E})$. The following example shows the existence of nonlinearity intervals and transition points.

EXAMPLE 1. Consider the following parametric SDO problem:

$$
\min \left\{ (4\epsilon - 2)x + (2 - 4\epsilon)y - 2z : \begin{pmatrix} 1 & x & y & 0 \\ x & 1 & z & 0 \\ y & z & 1 & 0 \\ 0 & 0 & 0 & 1-z \end{pmatrix} \succeq 0, \quad (x, y, z) \in \mathbb{R}^3 \right\},
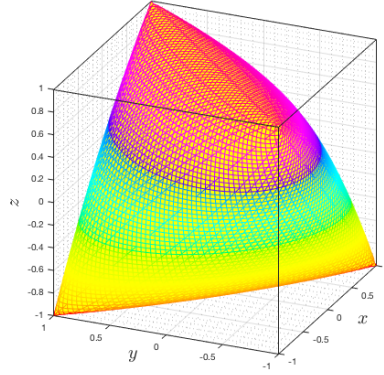\tag{6}
$$

FIGURE 1. The feasible set of the parametric SDO problem (6).

in which the feasible region is the intersection of a 3-elliptope and the inequality constraint $z \leq 1$, see Figure 1. Notice that (6) can be cast into the primal form (P_ϵ), where $X \in \mathbb{S}^4$ and $m = 7$.

It is easy to check that for all $\epsilon \in (-\frac{1}{2}, \frac{3}{2}) \setminus \{\frac{1}{2}\}$, see also [30, Example 3.1], the unique strictly complementary optimal solution of (6) is given by

$$
X^*(\epsilon) = \begin{pmatrix} 1 & \frac{1}{2} - \epsilon & \epsilon - \frac{1}{2} & 0 \\ \frac{1}{2} - \epsilon & 1 & 1 - 2(\epsilon - \frac{1}{2})^2 & 0 \\ \epsilon - \frac{1}{2} & 1 - 2(\epsilon - \frac{1}{2})^2 & 1 & 0 \\ 0 & 0 & 0 & 2(\epsilon - \frac{1}{2})^2 \end{pmatrix},
$$

$$
y^*(\epsilon) = \left(-(2\epsilon - 1)^2, -1, -1, 0, 0, 0, 0 \right)^T, \qquad S^*(\epsilon) = \begin{pmatrix} (2\epsilon - 1)^2 & 2\epsilon - 1 & 1 - 2\epsilon & 0 \\ 2\epsilon - 1 & 1 & -1 & 0 \\ 1 - 2\epsilon & -1 & 1 & 0 \\ 0 & 0 & 0 & 0 \end{pmatrix}, \tag{7}
$$

and the analytic center [15] of the optimal set at $\epsilon = \frac{1}{2}$ is given by

$$
X^*(\tfrac{1}{2}) = \begin{pmatrix} 1 & 0 & 0 & 0 \\ 0 & 1 & 1 & 0 \\ 0 & 1 & 1 & 0 \\ 0 & 0 & 0 & 0 \end{pmatrix}, \quad y^*(\tfrac{1}{2}) = \left(0, -\tfrac{1}{2}, -\tfrac{1}{2}, -1, 0, 0, 0 \right)^T, \quad S^*(\tfrac{1}{2}) = \begin{pmatrix} 0 & 0 & 0 & 0 \\ 0 & \frac{1}{2} & -\frac{1}{2} & 0 \\ 0 & -\frac{1}{2} & \frac{1}{2} & 0 \\ 0 & 0 & 0 & 1 \end{pmatrix}.
$$

The eigenvalue decompositions of $X^*(\epsilon)$ and $S^*(\epsilon)$ reveal that

$$
\mathrm{rank}\left(X^*(\epsilon) \right) = \begin{cases} 3 & \epsilon \in (-\frac{1}{2}, \frac{3}{2}) \setminus \{\frac{1}{2}\}, \\ 2 & \epsilon = \frac{1}{2}, \end{cases} \qquad \mathrm{rank}\left(S^*(\epsilon) \right) = \begin{cases} 1 & \epsilon \in (-\frac{1}{2}, \frac{3}{2}) \setminus \{\frac{1}{2}\}, \\ 2 & \epsilon = \frac{1}{2}. \end{cases}
$$

Thus, $(-\frac{1}{2}, \frac{1}{2})$ and $(\frac{1}{2}, \frac{3}{2})$ are nonlinearity intervals and $\epsilon = \frac{1}{2}$ is a transition point of the optimal partition. In fact, for all $\epsilon \in (-\frac{1}{2}, \frac{3}{2}) \setminus \{\frac{1}{2}\}$, the optimal partition is given by

$$
\mathcal{B}(\epsilon) = \mathcal{R}\left(\begin{pmatrix} 0 & \frac{2\mathrm{sgn}(2\epsilon-1)}{\sqrt{2(2\epsilon-1)^2+4}} & 0 \\ \frac{1}{\sqrt{2}} & \frac{-|2\epsilon-1|}{\sqrt{2(2\epsilon-1)^2+4}} & 0 \\ \frac{1}{\sqrt{2}} & \frac{|2\epsilon-1|}{\sqrt{2(2\epsilon-1)^2+4}} & 0 \\ 0 & 0 & 1 \end{pmatrix} \right), \quad \mathcal{T}(\epsilon) = \{0\}, \quad \mathcal{N}(\epsilon) = \mathcal{R}\left(\begin{pmatrix} \frac{(1-2\epsilon)}{\sqrt{(2\epsilon-1)^2+2}} \\ \frac{-1}{\sqrt{(2\epsilon-1)^2+2}} \\ \frac{1}{\sqrt{(2\epsilon-1)^2+2}} \\ 0 \end{pmatrix} \right),
$$

while the optimal partition at $\epsilon = \frac{1}{2}$ is

$$\mathcal{B}(\tfrac{1}{2}) = \mathcal{R}\left(\begin{pmatrix} 0 & 1 \\ \frac{1}{\sqrt{2}} & 0 \\ \frac{1}{\sqrt{2}} & 0 \\ 0 & 0 \end{pmatrix}\right), \quad \mathcal{T}(\tfrac{1}{2}) = \{0\}, \qquad \mathcal{N}(\tfrac{1}{2}) = \mathcal{R}\left(\begin{pmatrix} 0 & 0 \\ \frac{-1}{\sqrt{2}} & 0 \\ \frac{1}{\sqrt{2}} & 0 \\ 0 & 1 \end{pmatrix}\right),$$

where sgn(.) denotes the signum function.

Due to unknown behavior of the optimal set mapping in a parametric SDO problem, see Remark 2, a general existence condition for a nonlinearity interval or a transition point is still an open question. Nevertheless, strict complementarity coupled with the continuity of the optimal set mapping at a given $\bar{\epsilon}$ relative to int($\mathcal{E}$) provide sufficient conditions for the existence of a nonlinearity interval surrounding $\bar{\epsilon}$, see also [30, Theorems 3.7 and 3.10].

LEMMA 3.   *Assume that $\{\bar{\epsilon}\}$ is a singleton invariancy set. If $(X^*(\bar{\epsilon}), y^*(\bar{\epsilon}), S^*(\bar{\epsilon}))$ is a strictly complementary optimal solution, and both the primal and dual optimal set mappings are continuous at $\bar{\epsilon}$ relative to int($\mathcal{E}$), then $\bar{\epsilon}$ belongs to a nonlinearity interval.*

Proof The strict complementarity condition yields

$$\text{rank}\big(X^*(\bar{\epsilon})\big) + \text{rank}\big(S^*(\bar{\epsilon})\big) = n.$$

Continuity of $X^*(\epsilon)$ and $S^*(\epsilon)$ at $\bar{\epsilon}$, along with the continuity of the eigenvalues, shows that $\text{rank}\big(X^*(\bar{\epsilon})\big) \leq \text{rank}\big(X^*(\epsilon)\big)$ and $\text{rank}\big(S^*(\bar{\epsilon})\big) \leq \text{rank}\big(S^*(\epsilon)\big)$ for all ϵ in a small neighborhood of $\bar{\epsilon}$, see also [36, Theorem 3B.2(b)]. Hence, the rank of $X^*(\epsilon)$ and $S^*(\epsilon)$ remain constant on a sufficiently small neighborhood of $\bar{\epsilon}$. □

Unfortunately, the converse of Lemma 3 is not necessarily true for a parametric SDO problem. In fact, the primal or dual optimal set mapping might fail to be continuous on a nonlinearity interval. This can occur since the lim inf of a sequence of faces is not necessarily a face of the feasible set, i.e., it might be a subset of the relative interior of a face. A counterexample can be given as

$$\min\left\{(4\epsilon - 2)x + (2 - 4\epsilon)y - 2z : \begin{pmatrix} 1 & x & y \\ x & 1 & z \\ y & z & 1 \end{pmatrix} \succeq 0, \quad (x, y, z) \in \mathbb{R}^3\right\}, \tag{8}$$

where the strict complementarity condition holds on a nonlinearity interval $(-\frac{1}{2}, \frac{3}{2})$, see [30, Example 3.1]. The primal optimal set mapping is single-valued, and thus continuous, everywhere on $(-\frac{1}{2}, \frac{1}{2}) \cup (\frac{1}{2}, \frac{3}{2})$. However, $\mathcal{P}^*(\epsilon)$ fails to be inner semicontinuous at $\epsilon = \frac{1}{2}$, because

$$\liminf_{k \to \infty} \mathcal{P}^*(\epsilon_k) \subset \text{ri}(\mathcal{P}^*(\tfrac{1}{2}))$$

for any sequence $\epsilon_k \to \frac{1}{2}$.

REMARK 3.   The continuity condition in Lemma 3 can be relaxed by imposing the conditions

$$\liminf_{k \to \infty} \mathcal{P}^*(\epsilon_k) \cap \text{ri}\big(\mathcal{P}^*(\bar{\epsilon})\big) \neq \emptyset \quad \text{and} \quad \liminf_{k \to \infty} \mathcal{D}^*(\epsilon_k) \cap \text{ri}\big(\mathcal{D}^*(\bar{\epsilon})\big) \neq \emptyset \tag{9}$$

for every sequence $\epsilon_k \to \bar{\epsilon}$, see also [36, Proposition 3A.1], which by (2) and the continuity of the eigenvalues imply the existence of a nonlinearity interval around $\bar{\epsilon}$. However, even the weaker
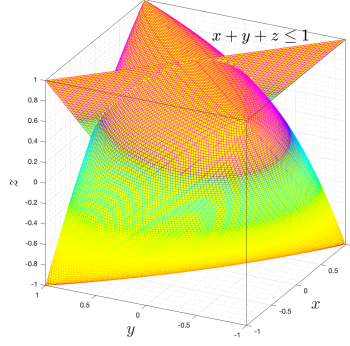
FIGURE 2. The feasible set of the parametric SDO problem (10).

condition (9) may not hold on a nonlinearity interval. For instance, by adding the inequality constraint $x + y + z \leq 1$ to (8) we get

$$\min \left\{ (4\epsilon - 2)x + (2 - 4\epsilon)y - 2z : \begin{pmatrix} 1 & x & y & 0 \\ x & 1 & z & 0 \\ y & z & 1 & 0 \\ 0 & 0 & 0 & 1-x-y-z \end{pmatrix} \succeq 0, \quad (x,y,z) \in \mathbb{R}^3 \right\}, \qquad (10)$$

for which $\left(X^*(\epsilon), y^*(\epsilon), S^*(\epsilon)\right)$ defined by (7) is still a unique strictly complementary optimal solution for all $\epsilon \in (-\frac{1}{2}, \frac{3}{2}) \setminus \{\frac{1}{2}\}$, see Figure 2. However, for any $\epsilon_k \to \frac{1}{2}$ the sequence $X^*(\epsilon_k)$ converges to an optimal solution on the boundary of $\mathcal{P}^*(\frac{1}{2})$. This example shows that even a continuous selection [37, Chapter 5(J)] through the relative interior of the optimal sets might fail to exist on a nonlinearity interval. However, we do not know yet whether (9) could fail at a boundary point of a nonlinearity interval.

4. Identification of the optimal partitions This section proposes a methodology to identify the optimal partitions on the entire $\text{int}(\mathcal{E})$. By Definitions 3 to 5, the interval $\text{int}(\mathcal{E})$ is the union of invariancy intervals, nonlinearity intervals, and transition points. An invariancy interval can be efficiently computed by solving the auxiliary problems (4). In general, however, the identification of a nonlinearity interval around a given $\bar{\epsilon}$ is a nontrivial computational task, since the conditions of Lemma 3 may not be easily checked in practice. One could try to simply solve (P$_\epsilon$) and (D$_\epsilon$) for various ϵ in a neighborhood of $\bar{\epsilon}$ with the aim of finding the desired nonlinearity interval. However, this could fail due to the fact that the solution of IPMs usually come with numerical inaccuracy, while an eigenvalue of $X^*(\epsilon)$ or $S^*(\epsilon)$ might be doubly exponentially small [34]. On the other hand, since the set of transition points might have empty interior, see Lemma 2, the numerical inaccuracy could lead one to miss a transition point when simply solving (P$_\epsilon$) and (D$_\epsilon$) at a given set of mesh points.

In order to compute the nonlinearity intervals, we numerically locate the transition points by reformulating the optimality conditions (1) as a system of polynomials. We then view the problem of finding transition points through the lens of numerical algebraic geometry, see [7, 39] for an overview of results regarding polynomial systems. Together with the auxiliary problems (4), this approach allows us to identify the optimal partitions on $\text{int}(\mathcal{E})$.

4.1. Algebraic formulation For $\mathcal{A} := \big(\text{svec}(A^1), \ldots, \text{svec}(A^m)\big)^T$, the optimality conditions (1) can be equivalently written as

$$F(V, \epsilon) := \begin{pmatrix} \mathcal{A}\,\text{svec}(X) - b \\ \mathcal{A}^T y + \text{svec}(S) - \text{svec}(C + \epsilon \bar{C}) \\ \frac{1}{2}\,\text{svec}(XS + SX) \end{pmatrix} = 0, \tag{11}$$

$$X, S \succeq 0, \tag{12}$$

where $V := (X, y, S)$ is the vector of variables. Given a particular ϵ, the set of solutions satisfying (11) is denoted by

$$\mathbf{V}\big(F(V, \epsilon)\big) := \big\{V \in \mathbb{C}^{m+2n} : F(V, \epsilon) = 0\big\}. \tag{13}$$

Following this notation, a solution in $\mathbf{V}\big(F(V, \epsilon)\big)$, an optimal solution, and a maximally complementary optimal solution of (P_ϵ) and (D_ϵ) are denoted by $\underline{V}(\epsilon)$, $V(\epsilon)$, and $V^*(\epsilon)$, respectively. Clearly, $\underline{V}(\epsilon)$ is not necessarily an optimal solution of (P_ϵ) and (D_ϵ). As ϵ varies on a nonlinearity interval $\mathcal{I}_{\text{non}}$, the solutions $V^*(\epsilon)$ for $\epsilon \in \mathcal{I}_{\text{non}}$ form a *solution sheet* of (11).

The Jacobian matrix of (11) is given by

$$J(V, \epsilon) := \begin{pmatrix} \mathcal{A} & 0 & 0 \\ 0 & \mathcal{A}^T & I_{n(n+1)/2} \\ S \otimes_s I_n & 0 & X \otimes_s I_n \end{pmatrix},$$

where the symmetric Kronecker product $\otimes_s$ is defined in Section 1.4. If the Jacobian is nonsingular at $(V^*(\bar{\epsilon}), \bar{\epsilon})$, then $V^*(\bar{\epsilon})$ is the unique and strictly complementary optimal solution of $(\text{P}_{\bar{\epsilon}})$ and $(\text{D}_{\bar{\epsilon}})$.

LEMMA 4 **(Theorem 3.1 of [2] and [20])**. *The Jacobian $J\big(V^*(\bar{\epsilon}), \bar{\epsilon}\big)$ is nonsingular if and only if the optimal solution $V^*(\bar{\epsilon})$ is unique and strictly complementary.*

When the Jacobian is nonsingular, then the implicit function theorem [36] and Lemma 3 describe the behavior of $V^*(\epsilon)$ in a neighborhood of $\bar{\epsilon}$ and induce the existence of a nonlinearity interval around $\bar{\epsilon}$, see [30, Lemma 3.9] and the subsequent discussion therein. Consequently, transition points and the points at which $\mathcal{P}^*(\epsilon)$ or $\mathcal{D}^*(\epsilon)$ fails to be continuous relative to $\text{int}(\mathcal{E})$ are both subsets of *singular points*, i.e., the set of $\epsilon \in \mathbb{C}$ such that

$$\exists\, \underline{V}(\epsilon) \in \mathbf{V}\big(F(V, \epsilon)\big) \text{ where } J\big(\underline{V}(\epsilon), \epsilon\big) \text{ is singular},$$

in which case $\underline{V}(\epsilon)$ is called a *singular solution*. This inclusion might be strict as demonstrated by problem (8), where $\epsilon = \frac{1}{2}$ is a singular point but not a transition point. If ϵ is not a singular point, then it is called a *nonsingular point*. Here, our goal is to locate the real singular points in $\text{int}(\mathcal{E})$ and then identify the transition points out of the singular points.

Singular points of parameterized systems are well-studied in algebraic geometry, e.g., Sylvester's 19th century work in discriminants and resultants [40, 41]. Under a mild assumption, the algebraic formulation (11) shows that the set of singular points must be an algebraic subset of $\mathbb{C}$, leading to the following finiteness result.

THEOREM 2. *Assume that there exists a nonsingular point $\bar{\epsilon} \in \text{int}(\mathcal{E})$. Then the set of singular points in $\text{int}(\mathcal{E})$, and hence the set of transition points and the set of points at which $\mathcal{P}^*(\epsilon)$ or $\mathcal{D}^*(\epsilon)$ fails to be continuous relative to $\text{int}(\mathcal{E})$, are finite.*

Proof By definition, the set Υ of all $(\underline{V}(\epsilon), \epsilon)$ with a singular Jacobian satisfies

$$\Upsilon := \big\{ (V, \epsilon) \in \mathbb{C}^{m+2n+1} : F(V, \epsilon) = 0, \ \det\big(J(V, \epsilon)\big) = 0 \big\}, \tag{14}$$

where (14) is a basic constructible set [3] in $\mathbb{C}^{m+2n+1}$. Since the projection of a constructible set to $\mathbb{C}$ is a constructible subset of $\mathbb{C}$ [3, Theorem 1.22], it holds that

$$\big\{ \epsilon \in \mathbb{C} : \exists V \in \mathbb{C}^{m+2n} \ \text{s.t.} \ (V, \epsilon) \in \Upsilon \big\} \tag{15}$$

is either finite or the complement of a finite subset of $\mathbb{C}$, see e.g., [3, Exercise 1.2]. On the other hand, it follows from the assumption and the implicit function theorem that the complement of (15) contains an open neighborhood of $\bar{\epsilon}$. All this implies that the projection of Υ is finite, and thus it is an algebraic subset of $\mathbb{C}$. The finiteness result naturally holds when we restrict the set of singular points to $\mathbb{R}$, in which our domain $\mathcal{E}$ is defined. Consequently, there are only finitely many real singular points in $\mathrm{int}(\mathcal{E})$. $\quad\square$

REMARK 4. Under the weaker assumption that there exists a singular point $\epsilon \in \mathrm{int}(\mathcal{E})$ such that $J\big(V^*(\epsilon), \epsilon\big)$ is nonsingular, Theorem 2 implies the existence of finitely many singular solutions in the solution sheet which passes through $V^*(\epsilon)$.

From a computational algebraic geometry viewpoint, the problem of computing singular points for a parametric SDO problem was studied by the first and third authors in [24] in a more general context. Here, we present a simplified process to locate the singular points in $\mathrm{int}(\mathcal{E})$. To that end, we make the following assumption from this point on:

ASSUMPTION 2. *There exists a nonsingular point* $\bar{\epsilon} \in \mathrm{int}(\mathcal{E})$.

REMARK 5. While the condition of Lemma 2 automatically follows from Assumption 2, Theorem 2 provides a stronger result of finiteness.

With Assumption 2, it follows from Theorem 2 that any two invariancy/nonlinearity intervals are separated by a transition point. This will enable us to decompose $\mathrm{int}(\mathcal{E})$ into the union of finitely many open intervals of maximal length and their finitely many singular boundary points. The final step is to classify the singular points into transition and non-transition points and then form the nonlinearity intervals from the appropriate open intervals.

Given a nonsingular initial point $\bar{\epsilon} \in \mathrm{int}(\mathcal{E})$, the key idea is using Davidenko's [14, 28] ordinary differential equation (ODE)

$$J(V, \epsilon) \frac{dV}{d\epsilon} + \frac{\partial F(V, \epsilon)}{\partial \epsilon} = 0 \tag{16}$$

to track an optimal solution $V(\epsilon)$ from $\bar{\epsilon}$ to the nearest singular point in each direction. Since solutions of (16) correspond to level sets of $F(V, \epsilon)$, i.e., $\{(V, \epsilon) : F(V, \epsilon) = c\}$ for arbitrary constant c, using the initial condition $V(\bar{\epsilon}) = V^*(\bar{\epsilon})$ yields the set of solutions to (11) and (12) for all ϵ in a neighborhood of $\bar{\epsilon}$. Hence, this approach utilizes the local information provided by the Jacobian, when it is nonsingular, to obtain accurate approximations of the optimal solutions nearby. The following lemma provides a summary of the solution [24].

LEMMA 5 (**Theorems 2 and 3 in [24]**). *Suppose that the Jacobian is nonsingular on an interval* $\mathcal{I}_{\mathrm{reg}} \subseteq \mathrm{int}(\mathcal{E})$ *and let* $\bar{\epsilon} \in \mathcal{I}_{\mathrm{reg}}$. *Then,* $V^*(\epsilon)$ *is analytic on* $\mathcal{I}_{\mathrm{reg}}$, *and it is the unique solution of*

$$\frac{dV}{d\epsilon} = -J(V, \epsilon)^{-1} \frac{\partial F(V, \epsilon)}{\partial \epsilon}, \qquad V(\bar{\epsilon}) = V^*(\bar{\epsilon})$$

for every $\epsilon \in \mathcal{I}_{\mathrm{reg}}$.

Using the results of [22], we can track along $\mathcal{I}_{\text{reg}}$, on which the optimal solution $V^*(\epsilon)$ is analytic, until we reach the boundary points of $\mathcal{I}_{\text{reg}}$. As the perturbation parameter approaches a singular point at the boundary of $\mathcal{I}_{\text{reg}}$, ill-conditioning of $F(V, \epsilon) = 0$, or spurious numerical behavior will be detected numerically. Thus, the singularity of the Jacobian matrix $J(V, \epsilon)$ indicates the existence of a possible transition point. Consequently, the common scenario of jumping over a transition point, when using just an IPM on discrete mesh points, can be avoided.

At a singular boundary point $\hat{\epsilon}$, we examine the uniqueness of the corresponding optimal solution $V^a(\hat{\epsilon})$, where $V^a(\hat{\epsilon})$ is an accumulation point of the sequence of unique optimal solutions $V^*(\epsilon)$, obtained from (16), as $\epsilon \nearrow \hat{\epsilon}$ or $\epsilon \searrow \hat{\epsilon}$. An accumulation point exists, by the outer semicontinuity of $\mathcal{P}^*(\epsilon)$ and $\mathcal{D}^*(\epsilon)$ relative to $\text{int}(\mathcal{E})$, and it belongs to $\mathcal{P}^*(\hat{\epsilon}) \times \mathcal{D}^*(\hat{\epsilon})$. Toward this end, we compute the local dimension of the algebraic set $\mathbf{V}\big(F(V, \hat{\epsilon})\big)$ at $V^a(\hat{\epsilon})$ using a numerical local dimension test [4, 42]. The local dimension is defined as the maximum dimension of the irreducible components of $\mathbf{V}\big(F(V, \hat{\epsilon})\big)$ which contain $V^a(\hat{\epsilon})$. If $\mathbf{V}\big(F(V, \hat{\epsilon})\big)$ has local dimension zero at $V^a(\hat{\epsilon})$, then we can conclude from Lemma 3 that $\hat{\epsilon}$ is a transition point, since $V^a(\hat{\epsilon})$ turns out to be the unique optimal solution of $(\text{P}_{\hat{\epsilon}})$ and $(\text{D}_{\hat{\epsilon}})$. Otherwise, we need to examine the change of rank at a maximally complementary optimal solution $V^*(\hat{\epsilon})$. Such a solution is generic on the irreducible component of $\mathbf{V}\big(F(V, \hat{\epsilon})\big)$ which contains $V^a(\hat{\epsilon})$, and it can be computed efficiently using numerical algebraic geometry [7]. See e.g., [39] for a detailed description of algebraic sets and irreducible components.

4.2. Partitioning algorithm   Based on the above description, we present the outline of Algorithm 1, a three-part algorithm, i.e., Algorithms 2, 3 and 4, which partitions $\text{int}(\mathcal{E})$ into the finite union of invariancy intervals, nonlinearity intervals, and transition points. Algorithm 2 computes the singular boundary points of an invariancy interval, which are indeed the transition points in $\text{int}(\mathcal{E})$, by solving the auxiliary problems (4). Algorithm 3 locates the singular points in $\text{int}(\mathcal{E})$. In particular, Algorithm 3 tracks the optimal solution of (P_ϵ) and (D_ϵ) by solving the ODE system (16) using a predictor-corrector tracking method [12]. This procedure is repeated alongside Algorithm 2 until all singular points and invariancy intervals in $\text{int}(\mathcal{E})$ are identified. Finally, Algorithm 4 classifies the singular points into transition and non-transition points.

In order to completely cover the interval, the increment change $\Delta\epsilon$ can be positive or negative to allow both left and right movements from the starting point. Furthermore, we assume, for the simplicity of computation, that the domain $\mathcal{E}$ is bounded, i.e., $\mathcal{E} = [\mathcal{E}_{\min}, \mathcal{E}_{\max}]$, where $|\mathcal{E}_{\min}|, |\mathcal{E}_{\max}| < \infty$. Accordingly, the optimal value of the auxiliary problems (4) is constrained to $(\mathcal{E}_{\min}, \mathcal{E}_{\max})$.

Computation of singular points and invariancy intervals   Lemma 5 specifies a systematic way to approximate the boundary points of the nonsingular interval $\mathcal{I}_{\text{reg}}$ surrounding the given $\bar{\epsilon}$. The numerical detection of singular points is described in detail in [24] with respect to several singularity criteria, e.g., the derivative of $\lambda_{\min}\big(X^*(\epsilon)\big)$ and $\lambda_{\min}\big(S^*(\epsilon)\big)$ with respect to ϵ, or the singularity of the Jacobian of (11). We omit the details here and refer the reader to [24] for more information on the numerical implementation of the singularity criteria.

Once a singular point is identified, the numerical solution obtained from the ODE system (16) at the next mesh point is most likely non-optimal, due to the numerical instability or the infeasibility of the solution. Thus, we invoke a primal-dual IPM in Algorithms 2 and 3 to compute the unique optimal solution at the first neighboring mesh point in the remaining interval. In order to guarantee that every singular point is correctly identified, a finer mesh pattern might be needed, and a higher precision might be required for the computation of singular points, far beyond the double precision arithmetic.

Algorithm 1 Partitioning of $\mathrm{int}(\mathcal{E})$

Input: $\mathcal{A}$, b, C, $\bar{C}$, domain $[\mathcal{E}_{\min}, \mathcal{E}_{\max}]$, nonsingular initial point $\epsilon_{\mathrm{init}} \in \mathrm{int}(\mathcal{E})$, a positive increment change $\Delta\epsilon$

Output: The union $\mathcal{U}_{\mathrm{inv}}$ of invariancy intervals in $(\mathcal{E}_{\min}, \mathcal{E}_{\max})$, the union $\mathcal{U}_{\mathrm{non}}$ of nonlinearity intervals in $(\mathcal{E}_{\min}, \mathcal{E}_{\max})$, the set $\mathcal{U}_{\mathrm{tran}}$ of transition points in $(\mathcal{E}_{\min}, \mathcal{E}_{\max})$

Set $\epsilon = \epsilon_{\mathrm{init}}$, $\mathcal{U}_{\mathrm{inv}} = \emptyset$, $\mathcal{U}_{\mathrm{non}} = (\mathcal{E}_{\min}, \mathcal{E}_{\max})$, $\mathcal{U}_{\mathrm{tran}} = \emptyset$, and $\mathcal{U}_{\mathrm{sin}} = \emptyset$

while $\epsilon < \mathcal{E}_{\max}$ **do**   ▷ Track forwards
    repeat   ▷ Check the existence of an invariancy interval
        Set $(\alpha_{\mathrm{inv}}, \beta_{\mathrm{inv}}, \epsilon, \mathcal{U}_{\mathrm{inv}}, \mathcal{U}_{\mathrm{non}}, \mathcal{U}_{\mathrm{tran}}) = \mathrm{INVARIANCY}(\mathcal{A}, b, C, \bar{C}, \Delta\epsilon, \epsilon, \mathcal{E}_{\min}, \mathcal{E}_{\max}, \mathcal{U}_{\mathrm{inv}}, \mathcal{U}_{\mathrm{non}}, \mathcal{U}_{\mathrm{tran}})$
    until $\alpha_{\mathrm{inv}} < \beta_{\mathrm{inv}}$ and $\epsilon < \mathcal{E}_{\max}$

    if $\epsilon < \mathcal{E}_{\max}$ **then**
        Set $(\epsilon, \mathcal{U}_{\mathrm{inv}}, \mathcal{U}_{\mathrm{non}}, \mathcal{U}_{\mathrm{sin}}, \mathcal{U}_{\mathrm{tran}}) = \mathrm{SINGULAR}(\mathcal{A}, b, C, \bar{C}, \Delta\epsilon, \epsilon, \mathcal{U}_{\mathrm{inv}}, \mathcal{U}_{\mathrm{non}}, \mathcal{U}_{\mathrm{sin}}, \mathcal{U}_{\mathrm{tran}})$ ▷ Algorithm 3
    end if
end while

Set $\epsilon_0 = \begin{cases} \displaystyle\inf_{\epsilon \in \mathcal{U}_{\mathrm{inv}}} \epsilon & \mathcal{U}_{\mathrm{inv}} \neq \emptyset \\ \infty & \mathcal{U}_{\mathrm{inv}} = \emptyset \end{cases}$

Set $\epsilon = \min\{\epsilon_{\mathrm{init}}, \epsilon_0\}$

if $\epsilon > \mathcal{E}_{\min}$ **then**
    Set $\Delta\epsilon = -\Delta\epsilon$

    if $\epsilon < \epsilon_{\mathrm{init}}$ **then**   ▷ Move past a transition point
        Set $\epsilon = \epsilon + \Delta\epsilon$
    end if

    while $\epsilon > \mathcal{E}_{\min}$ **do**   ▷ Track backwards
        repeat   ▷ Check the existence of an invariancy interval
            Set $(\alpha_{\mathrm{inv}}, \beta_{\mathrm{inv}}, \epsilon, \mathcal{U}_{\mathrm{inv}}, \mathcal{U}_{\mathrm{non}}, \mathcal{U}_{\mathrm{tran}}) = \mathrm{INVARIANCY}(\mathcal{A}, b, C, \bar{C}, \Delta\epsilon, \epsilon, \mathcal{E}_{\min}, \mathcal{E}_{\max}, \mathcal{U}_{\mathrm{inv}}, \mathcal{U}_{\mathrm{non}}, \mathcal{U}_{\mathrm{tran}})$
        until $\alpha_{\mathrm{inv}} < \beta_{\mathrm{inv}}$ and $\epsilon > \mathcal{E}_{\min}$

        if $\epsilon > \mathcal{E}_{\min}$ **then**
            Set $(\epsilon, \mathcal{U}_{\mathrm{inv}}, \mathcal{U}_{\mathrm{non}}, \mathcal{U}_{\mathrm{sin}}, \mathcal{U}_{\mathrm{tran}}) = \mathrm{SINGULAR}(\mathcal{A}, b, C, \bar{C}, \Delta\epsilon, \epsilon, \mathcal{U}_{\mathrm{inv}}, \mathcal{U}_{\mathrm{non}}, \mathcal{U}_{\mathrm{sin}}, \mathcal{U}_{\mathrm{tran}})$ ▷ Algorithm 3
        end if
    end while
end if

if $\{\epsilon : (V, \epsilon) \in \mathcal{U}_{\mathrm{sin}}\} \setminus \mathcal{U}_{\mathrm{tran}} \neq \emptyset$ **then**   ▷ Classify the singular points which are not already in $\mathcal{U}_{\mathrm{tran}}$
    Set $\mathcal{U}_{\mathrm{tran}} = \mathrm{TRANSITION}(\mathcal{U}_{\mathrm{sin}}, \mathcal{U}_{\mathrm{tran}})$ ▷ Algorithm 4
end if

Set $\mathcal{U}_{\mathrm{non}} = \mathcal{U}_{\mathrm{non}} \setminus \mathcal{U}_{\mathrm{tran}}$

Solution sharpening   Since the singular points are algebraic numbers, they can be computed to arbitrary accuracy, see e.g., [23]. The process of increasing the algebraic precision of a singular point is also known as the sharpening process, see Algorithm 3. More specifically, using a numerical approximation of a given singular point, which is indeed the nearest mesh point to the singular

---

Algorithm 2 Identification of invariancy intervals

---

function INVARIANCY($\mathcal{A}$, b, C, $\bar{C}$, $\Delta\epsilon$, ϵ, $\mathcal{E}_{\min}$, $\mathcal{E}_{\max}$, $\mathcal{U}_{\text{inv}}$, $\mathcal{U}_{\text{non}}$, $\mathcal{U}_{\text{tran}}$)
    Output: α_{inv}, β_{inv}, ϵ, $\mathcal{U}_{\text{inv}}$, $\mathcal{U}_{\text{non}}$, $\mathcal{U}_{\text{tran}}$

    Compute the unique optimal solution $V^*(\epsilon)$ using a primal-dual IPM

    Compute the orthonormal basis $Q_{\mathcal{N}(\epsilon)}$ from $V^*(\epsilon)$

    Using $Q_{\mathcal{N}(\epsilon)}$ solve the SDO problems (4) restricted to $(\mathcal{E}_{\min}, \mathcal{E}_{\max})$ to obtain α_{inv} and β_{inv}
    if $\alpha_{\text{inv}} < \epsilon < \beta_{\text{inv}}$ **then**
        Set $\mathcal{U}_{\text{inv}} = \mathcal{U}_{\text{inv}} \cup (\alpha_{\text{inv}}, \beta_{\text{inv}})$ and $\mathcal{U}_{\text{non}} = \mathcal{U}_{\text{non}} \setminus (\alpha_{\text{inv}}, \beta_{\text{inv}})$
        if $\alpha_{\text{inv}} > \mathcal{E}_{\min}$ and $\alpha_{\text{inv}} \notin \mathcal{U}_{\text{tran}}$ **then**
            Set $\mathcal{U}_{\text{tran}} = \mathcal{U}_{\text{tran}} \cup \{\alpha_{\text{inv}}\}$
        end if
        if $\beta_{\text{inv}} < \mathcal{E}_{\max}$ and $\beta_{\text{inv}} \notin \mathcal{U}_{\text{tran}}$ **then**
            Set $\mathcal{U}_{\text{tran}} = \mathcal{U}_{\text{tran}} \cup \{\beta_{\text{inv}}\}$
        end if
        if $\Delta\epsilon < 0$ **then**   ▷ Move past a transition point
            Set $\epsilon = \alpha_{\text{inv}} + \Delta\epsilon$
        else
            Set $\epsilon = \beta_{\text{inv}} + \Delta\epsilon$
        end if
    end if
end function

Algorithm 3 Identification of the singular points

---

function SINGULAR($\mathcal{A}$, b, C, $\bar{C}$, $\Delta\epsilon$, $\bar{\epsilon}$, $\mathcal{U}_{\text{inv}}$, $\mathcal{U}_{\text{non}}$, $\mathcal{U}_{\text{sin}}$, $\mathcal{U}_{\text{tran}}$)
    Output: ϵ, $\mathcal{U}_{\text{inv}}$, $\mathcal{U}_{\text{non}}$, $\mathcal{U}_{\text{sin}}$, $\mathcal{U}_{\text{tran}}$

    Set $F(V, \epsilon) = [\mathcal{A}\operatorname{svec}(X) - b; \mathcal{A}^T y + \operatorname{svec}(S) - \operatorname{svec}(C + \epsilon\bar{C}); \frac{1}{2}\operatorname{svec}(XS + SX)]$

    Compute the unique optimal solution $V^*(\bar{\epsilon})$ using a primal-dual IPM

    Set $\epsilon = \bar{\epsilon}$

    while $\epsilon + \Delta\epsilon \in \mathcal{U}_{\text{non}}$ and Jacobian is nonsingular on $[\epsilon, \epsilon + \Delta\epsilon]$ **do**   ▷ Check the singularity
        Set $\epsilon = \epsilon + \Delta\epsilon$
        Compute the unique optimal solution $V^*(\epsilon)$ by solving (16) with initial point $V^*(\bar{\epsilon})$
    end while

    if $\epsilon + \Delta\epsilon \in \mathcal{U}_{\text{non}}$ and a singular point exists in $[\epsilon, \epsilon + \Delta\epsilon]$ **then**   ▷ Compute the singular point
        Compute the singular point $\hat{\epsilon}$ and set $\mathcal{U}_{\text{sin}} = \mathcal{U}_{\text{sin}} \cup \{(V^a(\hat{\epsilon}), \hat{\epsilon})\}$
        Set $\epsilon = \hat{\epsilon} + \Delta\epsilon$ ▷ Move past a singular point
    else
        Set $\epsilon = \epsilon + \Delta\epsilon$
    end if
end function

---

point, the theory of isosingular sets [25] allows one to construct a new polynomial system where Newton's method would converge quadratically to the singular point.

Classification of singular points The use of adaptive precision, see e.g., [6], in `Bertini` [5, 7] ensures that adequate precision is being used for reliable computations near the singular solutions. This method enables one to compute a maximally complementary optimal solution near $V^a(\hat{\epsilon})$ to arbitrary accuracy. With the ability to refine the accuracy of a maximally complementary optimal solution, we can determine if a given singular point is a transition point. This can be done robustly by examining the rank of $X^*(\epsilon)$ and $S^*(\epsilon)$ using standard numerical rank revealing methods, such as singular value decomposition. More specifically, by computing the eigenvalues of an approximate maximally complementary optimal solution at various precisions, one can determine if the least positive eigenvalues of $X^*(\epsilon)$ and $S^*(\epsilon)$ converge to zero as we increase the precision of computation. This process accurately reveals the rank of $X^*(\epsilon)$ and $S^*(\epsilon)$ at a singular point.

Algorithm 4 Classification of the singular points

---

    function TRANSITION($\mathcal{U}_{\text{sin}}, \mathcal{U}_{\text{tran}}$)
        Output: $\mathcal{U}_{\text{tran}}$

        for $(V, \epsilon) \in \mathcal{U}_{\text{sin}}$ **do**
            Calculate the local dimension d of the algebraic set $\mathbf{V}\big(F(V, \epsilon)\big)$, defined in (13), at V
            if $d = 0$ **then**
                Set $\mathcal{U}_{\text{tran}} = \mathcal{U}_{\text{tran}} \cup \{\epsilon\}$
            else   ▷ Compute a maximally complementary optimal solution $V^*(\epsilon)$
                Use a polynomial solver to compute $V^*(\epsilon)$ in the irreducible component which contains V
                if the rank of $X^*(\epsilon)$ or $S^*(\epsilon)$ changes **then**
                    Set $\mathcal{U}_{\text{tran}} = \mathcal{U}_{\text{tran}} \cup \{\epsilon\}$
                end if
            end if
        end for
    end function

---

5. Numerical examples In this section, using the approach described in Section 4 and outlined by Algorithm 1, we conduct numerical experiments on the computation of nonlinearity intervals and transition points. Section 5.1 demonstrates the convergence rate of computing the singular points. Section 5.2 describes a parametric SDO problem where the continuity of the dual optimal set mapping fails at a transition point. Section 5.3 computes the nonlinearity interval of the parametric SDO problem (10) where the Jacobian is singular at a non-transition point. All numerical experiments are conducted on a PC with Intel Core i7-6500U CPU @2.5 GHz.

5.1. Convergence rate Consider the following parametric SDO problem

$$
\begin{aligned}
\min \quad & -2\epsilon x_1 - 2(1-\epsilon)x_2 \\
\text{s.t.} \quad & \begin{pmatrix} 1 & x_1 & x_2 & 0 & 0 \\ x_1 & 1 & 0 & 0 & 0 \\ x_2 & 0 & 1 & 0 & 0 \\ 0 & 0 & 0 & x_2 & x_1 - 1 \\ 0 & 0 & 0 & x_1 - 1 & x_2 \end{pmatrix} \succeq 0,
\end{aligned}
\tag{17}
$$

which can be cast into the primal form (P_ϵ), where $m = 13$ and $X \in \mathbb{S}^5$. The block structure of the matrix indicates that (17) is indeed an SDO reformulation of a parametric second-order conic

optimization problem with $\mathcal{E} = \mathbb{R}$, see also Figure 3. For computational purposes, we choose a bounded domain $[-\frac{1}{4}, \frac{5}{4}]$ and the initial point $\epsilon = \frac{1}{4}$, where $\text{rank}\left(X^*(\frac{1}{4})\right) = 4$ and $\text{rank}\left(S^*(\frac{1}{4})\right) = 1$.
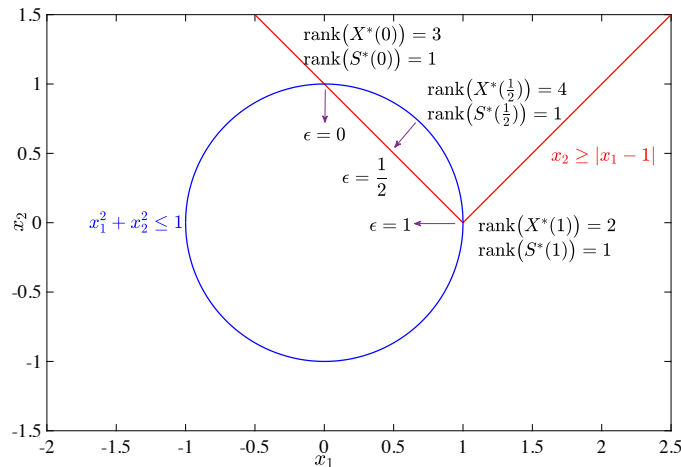

FIGURE 3. The feasible set of problem (17).

Algorithm 2 identifies $\epsilon = \frac{1}{4}$ as a singleton invariancy set belonging to a nonlinearity interval. We then invoke Algorithm 3 to track the unique optimal solutions until we locate the singular points $\epsilon = 0$ and $\epsilon = 1$. Algorithm 3 then computes a sufficiently accurate approximation of the singular points. Figure 4 demonstrates the exact and numerical approximation of $x_1(\epsilon)$ and the minimum modulus of the Jacobian eigenvalues versus ϵ. In particular, this tracking indicates that the Jacobian approaches singularity near $\epsilon = 0$ and $\epsilon = 1$.

Restarting at the first mesh point next to the singular points, Algorithm 2 identifies the invariancy intervals $(-\frac{1}{4}, 0)$ and $(1, \frac{5}{4})$ and determines that $\epsilon = 0$ and $\epsilon = 1$ are indeed the transition points of the optimal partition.

We should point out that while $J\left(V^*(\frac{1}{4}), \frac{1}{4}\right)$ is nonsingular, there exists a singular solution $\underline{V}(\frac{1}{4})$, and $J\left(V^*(\epsilon), \epsilon\right)$ is singular for every maximally complementary optimal solution $V^*(\epsilon)$ on $(-\infty, 0)$ and $(1, \infty)$. Nevertheless, Algorithm 1 produces the correct result even with the singular initial point $\epsilon = \frac{1}{4}$. In this case, by Remark 4, there are finitely many singular solutions in the solution sheet which passes through $V^*(\frac{1}{4})$.
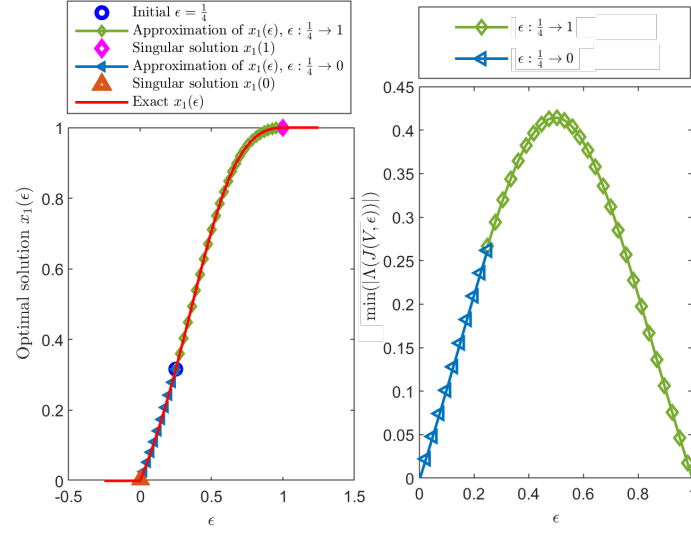
FIGURE 4. Left: The exact and numerical approximation of $x_1(\epsilon)$ versus ϵ. Right: The minimum modulus of the Jacobian eigenvalues.

Using different patterns of mesh points, we demonstrate the convergence of $x_1(\epsilon)$, computed by Algorithm 3, when ϵ approaches the singular points $\epsilon = 0$ and $\epsilon = 1$. To that end, we let initial $\Delta\epsilon$ take values from 0.05×2^{-j} for $j = 0, \ldots, 5$ or 0.03×2^{-j} for $j = 0, \ldots, 5$, and we set $\epsilon = \frac{1}{4}$ as the initial point. Tables 1 and 2 summarize the numerical results, where the L_1 error between the exact and numerical approximation of $x_1(\epsilon)$ on $[\frac{1}{4}, 1)$ and $(0, \frac{1}{4}]$, the order of convergence, and the computation time are reported. The order of convergence is computed by

$$\rho_{j+1} := \log_2\left(\frac{\text{Err}(\Delta\epsilon_j)}{\text{Err}(\Delta\epsilon_{j+1})}\right), \qquad j = 0, \ldots, 4,$$

where $\text{Err}(\Delta\epsilon_j)$ denotes the L_1 error associated with mesh pattern j. Notice the difference between ρ_j and the classical notion of the order of convergence in computational optimization.

TABLE 1. Convergence of $x_1(\epsilon)$ when ϵ approaches to the singular point $\epsilon = 1$.

j	$\Delta\epsilon_j$	Approximate singular point	$\text{Err}(\Delta\epsilon_j)$	ρ_j	CPU(s)
0	0.05	1.00	4.1597×10^{-6}	-	4.05
1	0.05×2^{-1}	1.00	2.6520×10^{-7}	3.971	6.56
2	0.05×2^{-2}	1.00	1.6707×10^{-8}	3.989	12.79
3	0.05×2^{-3}	1.00	1.0484×10^{-9}	3.994	26.14
4	0.05×2^{-4}	1.00	6.5671×10^{-11}	3.997	55.81
5	0.05×2^{-5}	1.00	4.1090×10^{-12}	3.998	125.27

In Table 1, the singular point $\epsilon = 1$ is exactly identified by Algorithm 3, since the singular point coincides with one of the mesh points. In general, however, it is unlikely that a singular point belongs to the mesh point set. This can be observed in Table 2, where a fixed increment change 0.03×2^{-j} for $j = 0, \ldots, 5$ is utilized. In this case, the approximate singular point is taken as the last mesh point before the minimum eigenvalues of $X^*(\epsilon)$ or $S^*(\epsilon)$, obtained from the ODE system (16),

become negative, or the first mesh point at which the minimum modulus of the Jacobian eigenvalues drops below 10^{-5}. As stated in Section 4.2, we can utilize numerical algebraic geometric tools to compute a singular point to arbitrary accuracy.

TABLE 2. Convergence of $x_1(\epsilon)$ when ϵ approaches to the singular point $\epsilon = 0$.

j	$\Delta\epsilon_j$	Approximate singular point	$\mathrm{Err}(\Delta\epsilon_j)$	ρ_j	CPU(s)
0	0.03	0.01	2.0415×10^{-7}	-	2.85
1	0.03×2^{-1}	0.01	1.2917×10^{-8}	3.982	4.57
2	0.03×2^{-2}	0.025	8.2444×10^{-10}	3.970	8.52
3	0.03×2^{-3}	0.0025	5.1677×10^{-11}	3.996	17.73
4	0.03×2^{-4}	0.000625	3.2461×10^{-12}	3.993	34.90
5	0.03×2^{-5}	0.000625	2.0302×10^{-13}	3.999	72.34

5.2. A transition point with discontinuous dual optimal set mapping We next consider the parametric SDO problem

$$\min \quad \epsilon x_1 + (1-\epsilon)x_2$$
$$\text{s.t.} \quad \begin{pmatrix} 1 & x_1 & x_2 & 0 & 0 & 0 \\ x_1 & 1 & 0 & 0 & 0 & 0 \\ x_2 & 0 & 1 & 0 & 0 & 0 \\ 0 & 0 & 0 & 1 & \frac{1}{2}x_1 & x_2 \\ 0 & 0 & 0 & \frac{1}{2}x_1 & 1 & 0 \\ 0 & 0 & 0 & x_2 & 0 & 1 \end{pmatrix} \succeq 0, \tag{18}$$

in which the feasible set is compact and $\mathcal{E} = \mathbb{R}$. It can be verified that the Jacobian is nonsingular on $\mathcal{E} \setminus \{0\}$, $\mathrm{rank}\big(X^*(\epsilon)\big) = 5$, and $\mathrm{rank}\big(S^*(\epsilon)\big) = 1$ at every $\epsilon \in \mathcal{E} \setminus \{0\}$. Since both the primal and dual problems have unique optimal solutions for every $\epsilon \in \mathcal{E} \setminus \{0\}$, the dual optimal set mapping fails to be continuous at $\epsilon = 0$.
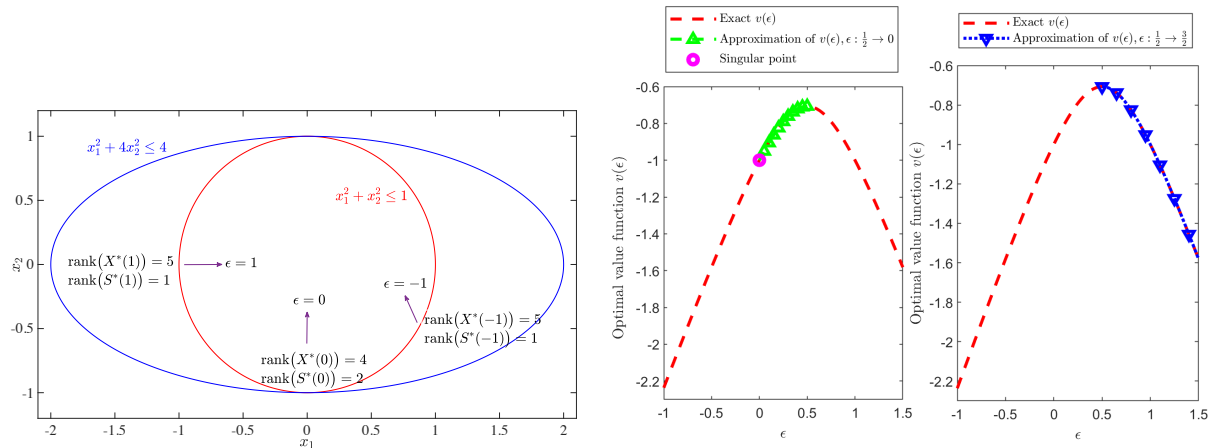

FIGURE 5. Left: The feasible set of problem (18). Right: The exact and numerical approximation of the optimal value function for problem (18) on $[-1, \frac{3}{2}]$.

For the purpose of numerical experiments, we consider the bounded domain $[-1, \frac{3}{2}]$. When starting from a nonsingular point $\epsilon = \frac{1}{2}$ with a fixed increment change 0.01, Algorithm 3 properly identifies

$\epsilon = 0$ as a singular point. One could easily skip over the singular point $\epsilon = 0$ when simply solving at a finite set of mesh points. Figure 5 demonstrates the exact optimal value function versus its numerical approximation obtained from Algorithm 3. Upon refining the accuracy of the approximate singular point and obtaining the singular point $\epsilon = 0$, we invoke `Bertini` solver in Algorithm 4 to compute the dimension of all irreducible components of $\mathbf{V}\big(F(V,0)\big)$ which contain $V^a(0)$. We observe that $V^a(0)$ lies on a 1-dimensional irreducible component of $\mathbf{V}\big(F(V,0)\big)$, and there exists a generic solution $V^*(0)$ such that $\mathrm{rank}\big(X^*(0)\big) = 4$ and $\mathrm{rank}\big(S^*(0)\big) = 2$. All this indicates that the rank of $X^*(\epsilon)$ and $S^*(\epsilon)$ change at $\epsilon = 0$, and thus $\epsilon = 0$ is a transition point. Consequently, we can partition $(-1, \frac{3}{2})$ into two nonlinearity intervals $(-1, 0)$ and $(0, \frac{3}{2})$ and the transition point $\{0\}$.

5.3. A non-transition point with singular Jacobian Here, we apply Algorithm 1 to identify the singular points and the transition points of the parametric SDO problem (10) in a bounded domain $[-1, 2]$. We initialize Algorithm 1 with the nonsingular point $\epsilon = 0$, see (7), and the initial increment change $\Delta\epsilon = 0.005$. While tracking forwards, Algorithm 3 computes the numerical approximation of the unique optimal solution until it locates the singular points $\epsilon = \frac{1}{2}$ and $\epsilon = \frac{3}{2}$. Then restarting the solution tracking at $\frac{3}{2} + \Delta\epsilon$, Algorithm 2 identifies the invariancy interval $(\frac{3}{2}, 2)$ and the transition point $\epsilon = \frac{3}{2}$. In an analogous fashion, while tracking backwards, Algorithm 3 and Algorithm 2 identify the singular point $\epsilon = -\frac{1}{2}$ and the invariancy interval $(-1, -\frac{1}{2})$, respectively. Figure 6 illustrates the exact and numerical approximation of the optimal value function, where the singular/transition points are represented by the dots marks.
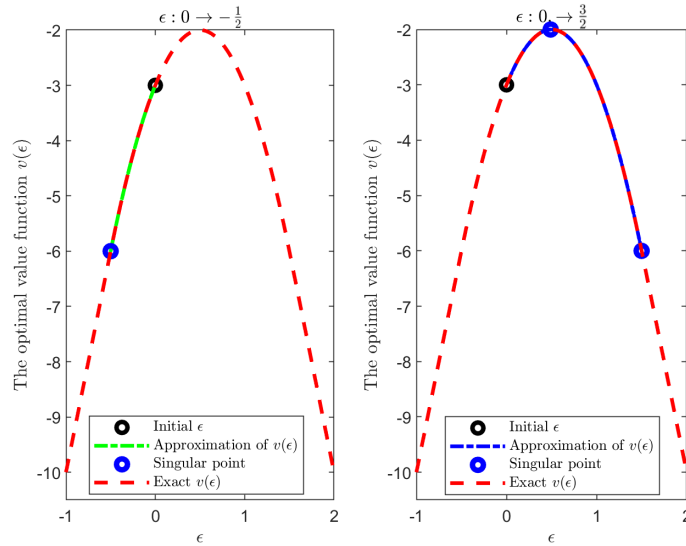

FIGURE 6. The exact and numerical approximation of the optimal value function for problem (10) on $[-1, 2]$.

Applying Algorithm 4 to the singular point $\epsilon = \frac{1}{2}$, we can observe that $V^a(\frac{1}{2})$ is not isolated, and it belongs to a 1-dimensional irreducible component of $\mathbf{V}\big(F(V, \frac{1}{2})\big)$. We then invoke the polynomial

solver `Bertini` to compute a generic solution

$$X^*(\tfrac{1}{2}) = \begin{pmatrix} 1 & -0.0449 & -0.0449 & 0 \\ -0.0449 & 1 & 1 & 0 \\ -0.0449 & 1 & 1 & 0 \\ 0 & 0 & 0 & 0.0898 \end{pmatrix}, \quad y^*(\tfrac{1}{2}) = \begin{pmatrix} 0 \\ -1 \\ -1 \\ 0 \\ 0 \\ 0 \\ 0 \end{pmatrix}, \quad S^*(\tfrac{1}{2}) = \begin{pmatrix} 0 & 0 & 0 & 0 \\ 0 & 1 & -1 & 0 \\ 0 & -1 & 1 & 0 \\ 0 & 0 & 0 & 0 \end{pmatrix},$$

in which $\mathrm{rank}\left(X^*(\tfrac{1}{2})\right) = 3$ and $\mathrm{rank}\left(S^*(\tfrac{1}{2})\right) = 1$. Given the rank of $X^*(\epsilon)$ and $S^*(\epsilon)$ on $(-\tfrac{1}{2}, \tfrac{1}{2}) \cup (\tfrac{1}{2}, \tfrac{3}{2})$, all this implies that the singular point $\epsilon = \tfrac{1}{2}$ belongs to the nonlinearity interval $(-\tfrac{1}{2}, \tfrac{3}{2})$. Consequently, the domain $(-1, 2)$ is partitioned as

$$\mathcal{U}_{\mathrm{inv}} = (-1, -\tfrac{1}{2}) \cup (\tfrac{3}{2}, 2), \quad \mathcal{U}_{\mathrm{non}} = (-\tfrac{1}{2}, \tfrac{3}{2}), \quad \mathcal{U}_{\mathrm{tran}} = \{-\tfrac{1}{2}, \tfrac{3}{2}\}.$$

6. Concluding remarks and future research This paper utilized an optimal partition approach to parametric analysis for SDO problems, where the objective function is perturbed along a fixed direction. In terms of continuity, we provided sufficient conditions for the existence of nonlinearity intervals and the emptiness of the interior of the set of transition points. We showed that the optimal set mapping might fail to be continuous on a nonlinearity interval, and the sequence of maximally complementary optimal solutions may converge to the boundary of the optimal set at an ϵ in a nonlinearity interval. Under the assumption of the existence of a nonsingular point in $\mathrm{int}(\mathcal{E})$, we then proposed a methodology, stemming from numerical algebraic geometry, to efficiently partition $\mathrm{int}(\mathcal{E})$ into finite union of invariancy intervals, nonlinearity intervals, and transition points. The computational approach was demonstrated on several examples.

We conjecture that condition (9) could fail at a boundary point of a nonlinearity interval. It is worth providing a counterexample or sufficient conditions which guarantee the validity of (9) at a boundary point of a nonlinearity interval. Furthermore, we still do not know about any upper bound on the number of points at which $\mathcal{P}^*(\epsilon)$ or $\mathcal{D}^*(\epsilon)$ fails to be continuous on a nonlinearity interval, or whether the subspaces $\left(\mathcal{B}(\epsilon), \mathcal{T}(\epsilon), \mathcal{N}(\epsilon)\right)$ move continuously on a nonlinearity interval. These topics are subjects of future research. We note that one could extend Theorem 2 to provide an upper bound on the number of singular points, and hence on the number of transition points. However, such bounds would be on the number of complex singular points, which may drastically overestimate the number of transition points in $\mathrm{int}(\mathcal{E})$.

References
[1] Adler I, Monteiro RDC (1992) A geometric view of parametric linear programming. *Algorithmica* 8(1):161–176.

[2] Alizadeh F, Haeberly JPA, Overton ML (1998) Primal-dual interior-point methods for semidefinite programming: Convergence rates, stability and numerical results. *SIAM Journal on Optimization* 8(3):746–768.

[3] Basu S, Pollack R, Roy MF (2006) *Algorithms in Real Algebraic Geometry* (Springer).

[4] Bates DJ, Hauenstein JD, Peterson C, Sommese AJ (2009) A numerical local dimensions test for points on the solution set of a system of polynomial equations. *SIAM Journal on Numerical Analysis* 47(5):3608–3623.

[5] Bates DJ, Hauenstein JD, Sommese AJ, Wampler CW (2006) Bertini: Software for Numerical Algebraic Geometry. Available at `bertini.nd.edu`.

[6] Bates DJ, Hauenstein JD, Sommese AJ, Wampler CW II (2008) Adaptive multiprecision path tracking. *SIAM Journal on Numerical Analysis* 46(2):722–746.

[7] Bates DJ, Sommese AJ, Hauenstein JD, Wampler CW (2013) *Numerically Solving Polynomial Systems with Bertini* (PA).

[8] Berkelaar A, Jansen B, Roos K, Terlaky T (1996) Sensitivity analysis in (degenerate) quadratic programming. Technical Report 96-26, Delft University of Technology, Netherlands.

[9] Bonnans JF, Ramírez C H (2005) Perturbation analysis of second-order cone programming problems. *Mathematical Programming* 104(2):205–227.

[10] Bonnans JF, Shapiro A (1998) Optimization problems with perturbations: A guided tour. *SIAM Review* 40(2):228–264.

[11] Bonnans JF, Shapiro A (2000) *Perturbation Analysis of Optimization Problems* (Springer).

[12] Butcher JC (2003) *Numerical Methods for Ordinary Differential Equations* (New York: John Wiley & Sons).

[13] Cifuentes D, Agarwal S, Parrilo P, Thomas R (2017) On the local stability of semidefinite relaxations. ArXiv:1710.04287 `https://arxiv.org/abs/1710.04287`.

[14] Davidenko D (1953) On a new method of numerical solution of systems of nonlinear eqauations. *Dokl. Akad. Nauk SSR* 87(4):601–602.

[15] de Klerk E (2006) *Aspects of Semidefinite Programming: Interior Point Algorithms and Selected Applications*, volume 65 of Series Applied Optimization (Springer).

[16] Fiacco A, McCormick G (1990) *Nonlinear Programming: Sequential Unconstrained Minimization Techniques*, volume 65 of the series Applied Optimization (SIAM).

[17] Fiacco AV (1976) Sensitivity analysis for nonlinear programming using penalty methods. *Mathematical Programming* 10(1):287–311.

[18] Fiacco AV (1983) *Introduction to Sensitivity and Stability Analysis in Nonlinear Programming*, volume 165 (Academic Press Inc.).

[19] Goldfarb D, Scheinberg K (1999) On parametric semidefinite programming. *Applied Numerical Mathematics* 29(3):361–377.

[20] Haeberly JP (1998) Remarks on nondegeneracy in mixed semidefinite-quadratic programming. Unpublished memorandum, available from `http://citeseerx.ist.psu.edu/viewdoc/download?doi=10.1.1.43.7501&rep=rep1&type=pdf`.

[21] Halická M, de Klerk E, Roos C (2002) On the convergence of the central path in semidefinite optimization. *SIAM Journal on Optimization* 12(4):1090–1099.

[22] Hauenstein JD, Haywood I, Liddell AC Jr (2014) An *a posteriori* certification algorithm for Newton homotopies. *ISSAC 2014—Proceedings of the 39th International Symposium on Symbolic and Algebraic Computation*, 248–255 (ACM, New York).

[23] Hauenstein JD, Sommese AJ (2017) What is numerical algebraic geometry? [Foreword]. *J. Symbolic Comput.* 79(part 3):499–507.

[24] Hauenstein JD, Tang T (2018) On semidefinite programming under perturbations with unknown boundaries Available at `https://www3.nd.edu/~jhauenst/preprints/htSDPperturb.pdf`.

[25] Hauenstein JD, Wampler CW (2013) Isosingular sets and deflation. *Foundations of Computational Mathematics* 13(3):371–403.

[26] Hogan WW (1973) Point-to-set maps in mathematical programming. *SIAM Review* 15(3):591–603.

[27] Jansen B, Roos K, Terlaky T (1993) An interior point method approach to postoptimal and parametric analysis in linear programming. Technical Report 92-21, Delft University of Technology, Netherlands.

[28] Kalaba RE, Zagustin E, Holbrow W, Huss R (1977) A modification of Davidenko's method for nonlinear systems. *Computers & Mathematics with Applications* 3(4):315–319.

[29] Kojima M (1980) Strongly stable stationary solutions in nonlinear programs. Robinson SM, ed., *Analysis and Computation of Fixed Points*, 93 – 138 (Academic Press).

[30] Mohammad-Nezhad A, Terlaky T (2018) Parametric analysis of semidefinite optimization. ArXiv:1808.00587 https://arxiv.org/abs/1808.00587.

[31] Munkres JR (2000) *Topology* (Prentice Hall).

[32] Nesterov Y, Nemirovskii A (1994) *Interior-Point Polynomial Algorithms in Convex Programming*, volume 13 (Society for Industrial and Applied Mathematics).

[33] Ortega J, Rheinboldt W (1970) *Iterative Solution of Nonlinear Equations in Several Variables*, volume 30 of Classics in Applied Mathematics (SIAM).

[34] Ramana MV (1997) An exact duality theory for semidefinite programming and its complexity implications. *Mathematical Programming* 77(1):129–162.

[35] Robinson SM (1982) Generalized equations and their solutions, part II: Applications to nonlinear programming. Guignard M, ed., *Optimality and Stability in Mathematical Programming*, 200–221 (Berlin, Heidelberg: Springer).

[36] Rockafellar R, Dontchev A (2014) *Implicit Functions and Solution Mappings* (Springer).

[37] Rockafellar RT, Wets RJB (2009) *Variational Analysis*, volume 317 (Springer).

[38] Shapiro A (1997) First and second order analysis of nonlinear semidefinite programs. *Mathematical Programming* 77(1):301–320.

[39] Sommese AJ, Wampler CW II (2005) *The numerical solution of systems of polynomials arising in engineering and science* (World Scientific Publishing Co. Pte. Ltd., Hackensack, NJ).

[40] Sylvester JJ (1851) On a remarkable discovery in the theory of canonical forms and of hyperdeterminants. *Philosophical Magazine* 4th series:391–410.

[41] Sylvester JJ (1904-1912) *The collected mathematical papers of James Joseph Sylvester* (Cambridge, England: Cambridge University press).

[42] Wampler CW, Hauenstein JD, Sommese AJ (2011) Mechanism mobility and a local dimension test. *Mechanism and Machine Theory* 46(9):1193–1206.

[43] Yildirim E (2004) Unifying optimal partition approach to sensitivity analysis in conic optimization. *Journal of Optimization Theory and Applications* 122(2):405–423.